Design of Folate-Linked Liposomal Doxorubicin to its Antitumor Effect in Mice

Atsushi Yamada,[1] Yukimi Taniguchi,[1] Kumi Kawano,[1] Takashi Honda,[2] Yoshiyuki Hattori,[1] and Yoshie Maitani[1]

Abstract

Purpose: Tumor cell targeting is a promising strategy for enhancing the therapeutic potential of chemotherapy agents. Polyethylene glycol (PEG)-coated (sterically stabilized) liposomes show enhanced accumulation on the surface of tumors, but steric hindrance by PEGylation reduces the association of the liposome-bound ligand with its receptor. To increase folate receptor (FR) targeting, we optimized the concentration and PEG spacer length of folate-PEG-lipid in liposomes.

Experimental Design: Three types of folate-linked liposomal doxorubicin were designed and prepared by optimizing the concentration and PEG spacer length of folate-PEG-lipid in PEGylated or non-PEGylated liposomes and by masking folate-linked liposomes where the folate ligand is "masked" by adjacent PEG spacers. The liposome targeting efficacy was evaluated *in vitro* and *in vivo*.

Results: In human oral carcinoma KB cells, which overexpress FR, modification with sufficiently long PEG spacer and a high concentration of folate ligand to non-PEGylated liposomes increased the FR-mediated association and cytotoxicity more than with PEGylated and masked folate-linked liposomes. On the contrary, in mice bearing murine lung carcinoma M109, modification with the folate ligand in PEGylated and masked folate-linked liposomes showed significantly higher antitumor effect than with non-PEGylated liposomes irrespective of the length of time in the circulation after intravenous injection.

Conclusions: The results of this study will be beneficial for the design and preparation of ligand-targeting carriers for cancer treatment.

A variety of targeting ligands have been examined in tumor-targeted drug carriers. Folate receptor (FR)-α is a glycosyl phosphatidylinositol-anchored membrane protein that is selectively overexpressed in >90% of ovarian carcinomas (1–3), and to various extents in other epithelial cancers, but is only minimally distributed in normal tissues (2, 4–6). FR can serve as an excellent tumor marker as well as a functional tumor-specific receptor. Folic acid, a high-affinity ligand for FR, retains its receptor-binding and endocytosis properties even if it is covalently linked to a wide variety of molecules. Therefore, liposomes conjugated to the folate ligand via a polyethylene glycol (PEG) spacer have been used to deliver chemotherapeutic agents, oligonucleotides, and markers to FR-bearing tumor cells (7–16). The targeting efficiency of folate-linked vesicles was affected by the amount of folate-PEG-lipid. It was reported that a higher molar fraction of folate-PEG-lipid in folate-linked liposomes reduced liposome uptake into cells (17). Folate molecules can form dimers, trimers, and even self-assembling tubular quartets at higher concentrations (18). Because FR can only bind one molecule of folic acid (19), such self-assembled multimers of folic acid are incapable of binding to FR.

PEGylated liposomes, called sterically stabilized liposomes, evade uptake by the reticuloendothelial system and show enhanced accumulation in tumors as a result of an enhanced permeability and retention effect. Liposomes were modified with folate to further increase targeting to FR and drug uptake by tumors. However, when targeting moieties are employed, circulation times are often decreased *in vivo* due to recognition by the reticuloendothelial system (9). As a result, the advantage of increased drug retention on the tumor surface by PEGylation is obscured by accelerated clearance of folate-linked formulations. Furthermore, steric hindrance by PEGylation reduces the association of the liposome-bound ligand with its receptor (8). Therefore, the density and PEG spacer length of the targeting ligand and PEGylation of liposomes are known to be critical characteristics for ligand-receptor interaction. However, there have been few studies concerned with the optimization of these factors.

In our previous studies, we have reported on the optimal folate concentration and PEG spacer length with nanoemulsions and polymer micelles (20, 21). However, in these cases,

Authors' Affiliations: [1]Institute of Medicinal Chemistry, Hoshi University, Tokyo, Japan and [2]Fukushima Medical University School of Nursing, Fukushima-City, Japan

Received 1/21/08; revised 5/16/08; accepted 6/6/08.

Grant support: Ministry of Education, Culture, Sports, Science and Technology, Japan, Ministry of Health, Labor and Welfare, Japan, and Open Research Center Project.

The costs of publication of this article were defrayed in part by the payment of page charges. This article must therefore be hereby marked *advertisement* in accordance with 18 U.S.C. Section 1734 solely to indicate this fact.

Note: Supplementary data for this article are available at Clinical Cancer Research Online (http://clincancerres.aacrjournals.org/).

Requests for reprints: Yoshie Maitani, Institute of Medicinal Chemistry, Hoshi University, Shinagawa, Ebara 2-4-41, Tokyo, 142-8501 Japan. Phone: 81-3-5498-5048; Fax: 81-3-5498-5048. E-mail: yoshie@hoshi.ac.jp.

doi:10.1158/1078-0432.CCR-08-0159

Translational Relevance

PEGylated liposomes show enhanced accumulation on the surface of tumors by long circulation. FR is selectively overexpressed to various extents in epithelial cancers. Folic acid is a high-affinity ligand for FR. The targeting efficiency of folate-linked vesicles was affected by the amount of both folate-PEG-lipid and PEG-lipid. To increase FR targeting, we optimized the concentration and PEG spacer length of folate-PEG-lipid in liposomes. In mice bearing murine lung carcinoma M109, modification with the folate ligand in PEGylated and masked folate-linked liposomes where the folate ligand is "masked" by adjacent PEG spacers showed significantly higher antitumor effect than with non-PEGylated liposomes after intravenous injection. This finding suggested that tumor targeting was achieved by less PEGylated carriers with ligand. Three anthracycline liposomal preparations including PEGylated liposomal doxorubicin (Doxil) are currently on the market, and many other liposomal formulations of antineoplastic drugs are in preclinical or clinical trials. Therefore, this strategy will be applied to such drug formulations for future practice of cancer medicine. The results of this study will be beneficial for the design and preparation of ligand-targeting carriers to deliver chemotherapeutic agents and gene for cancer treatment and contrast agents for the detection of solid tumors.

PEG-lipid and PEG polymer are the main components that form the nanoemulsions and polymer micelles, respectively, so we could not evaluate effect of folate-PEG-lipid alone on targeting to tumors. Because liposomes can be prepared without PEG-lipid, we can estimate the optimal density and PEG spacer length of folate-PEG-lipid for FR targeting to produce a balance between longer circulation time and FR targeting.

Here, we designed and prepared various folate-linked liposomes to increase the level of FR-targeting. In this study, we evaluated folate-mediated association of liposomal doxorubicin with human oral carcinoma KB cells and murine lung carcinoma M109 cells, which both overexpresses FR, in terms of the effect of PEG spacer length and the ratio of modification of the folate ligand of liposomes with or without PEG-coating and of the degree of masking of folate ligands on liposomes by adjacent PEG. Furthermore, the antitumor effect of these liposome preparations was investigated *in vitro* and *in vivo*.

Materials and Methods

Materials. Hydrogenated soybean phosphatidylcholine (HSPC) was obtained and amino-PEG-distearylphosphatidylethanolamine (amino-PEG-DSPE; PEG mean molecular weights, 2,000, 3,400, and 5,000) and methoxy-PEG-distearylphosphatidylethanolamine (mPEG-DSPE; PEG mean molecular weights, 2,000 and 5,000) were kind gifts from the NOF. Cholesterol, doxorubicin hydrochloride, and high-performance liquid chromatography-grade acetonitrile were purchased from Wako Pure Chemical Industries. Folate-PEG-DSPEs (F-PEG_{2000}-DSPE, F-PEG_{3400}-DSPE, and F-PEG_{5000}-DSPE), which are conjugates of folic acid and amino-PEG-DSPE, were synthesized as reported previously (8, 20). Folate-deficient RPMI 1640 and fetal bovine serum were obtained from Invitrogen. Other reagents used in this study were of reagent grade.

Preparation of folate-linked liposomal doxorubicin. Liposomes were prepared from hydrogenated soybean phosphatidylcholine/cholesterol = 55/45 (mol/mol) by a dry-film method. Briefly, all lipids were dissolved in chloroform, which was removed by evaporation. The thin film was hydrated with citrate buffer (300 mmol/L, adjusted to pH 4.0 with NaOH) at 60°C by vortex mixing and sonication. Targeted formulations were prepared by mixing nontargeted liposomes with micelles of mPEG-DSPE and/or F-PEG-DSPE to allow incorporation of targeting ligands at 60°C for 1 h by the postinsertion technique (22). The number of targeting ligands was controlled by altering the concentration of micelles added to the liposomes before loading with doxorubicin.

Schematic diagrams (Fig. 1) show three kinds of folate-PEG-liposomes: overhanging folate outside non-PEGylated liposomes (NL), PEGylated liposomes with a $mPEG_{2000}$ layer (SL), and masked folate inside a $mPEG_{5000}$ layer of liposomes (ML). NLs with folate ligands were prepared by incubation of NL with an aqueous dispersion of F-PEG-DSPE (from 0.01 to 0.5 mol% total lipids; Fig. 1A). SLs modified with folate were prepared by incubation of NLs with a total of 2.5 mol% PEG-lipids of $mPEG_{2000}$-DSPE and varying percentages of F-PEG_{5000}-DSPE (F5; Fig. 1B). MLs were prepared by incubation of NLs with an aqueous dispersion of 0.25 mol% F-PEG_{2000}-DSPE and 0.75 mol% $mPEG_{5000}$-DSPE (Fig. 1C). NLs linked with F-PEG_{2000}-DSPE, F-PEG_{3400}-DSPE, or F-PEG_{5000}-DSPE are henceforth abbreviated as F2-NL, F3-NL, and F5-NL, respectively, and SL linked with F-PEG_{5000}-DSPE is abbreviated as F5-SL. The number before the abbreviated term of F5-NL in some descriptions indicates the mol% F-PEG-DSPE of total lipids. For instance, 0.25F5-NL indicates liposomes with 0.25 mol% F-PEG_{5000}-DSPE of total lipids, and 0.25F5-SL indicates liposomes with total 2.5 mol% PEG-lipids composed of 2.25 mol% $mPEG_{2000}$-DSPE for steric stabilization and 0.25 mol% F-PEG_{5000}-DSPE. The resulting mean diameter and ζ potential of liposomes were determined by dynamic light scattering and electrophoresis methods, respectively (ELS-800; Otsuka Electronics) at 25°C after diluting the liposome suspension with water.

Next, these liposomes were actively loaded with doxorubicin by a pH gradient method (23). After the external pH was adjusted to pH 7.4, liposomes were incubated with doxorubicin [drug/lipid = 1:5 (w/w)] at 60°C for 25 min. Doxorubicin loading efficiency was determined by separating unencapsulated from encapsulated drug on a Sephadex G-50 column. Doxorubicin concentration was determined by measuring absorbance at 480 nm (UV-1700 Phamaspec; Shimadzu). The final liposomal doxorubicin was suspended in 150 mmol/L NaCl. The final total lipid concentration of folate-linked liposomes was 18.6 mg/mL.

In vitro ***drug release of liposomes.*** *In vitro* release of doxorubicin from the liposomal formulation was analyzed by membrane dialysis against PBS (pH 7.4) at 37°C under sink condition. Briefly, 1 mL liposomal doxorubicin (0.2 mg/mL doxorubicin) was placed in a dialysis tube (seamless cellulose tube membranes; Viskase Sales) with a molecular weight cutoff of 12,000 to 14,000 and then suspended in a temperature-controlled, jacketed flask containing 100 mL PBS. After various time intervals, aliquots of the medium were withdrawn. The doxorubicin concentration was analyzed using a fluorophotometer (Wallac 1420 ARVOsx multilabel counter; Perkin-Elmer Life Science) with excitation and emission wavelengths of 485 and 535 nm, respectively.

Cell culture. KB cells were obtained from the Cell Resource Center for Biomedical Research, Tohoku University. The human lung adenocarcinoma A549 cell line [FR(-)] was kindly provided by OncoTherapy Science. The cells were cultured in folate-deficient RPMI 1640 with 10% heat-inactivated fetal bovine serum and 50 μg/mL kanamycin sulfate in a humidified atmosphere containing 5% CO_2 at 37°C. The cells were prepared by plating 3×10^5 per well in a 12-well culture plate for flow cytometry analysis or 1×10^4 per well in a 96-well culture plate for cytotoxicity analysis for 1 day before the assay.

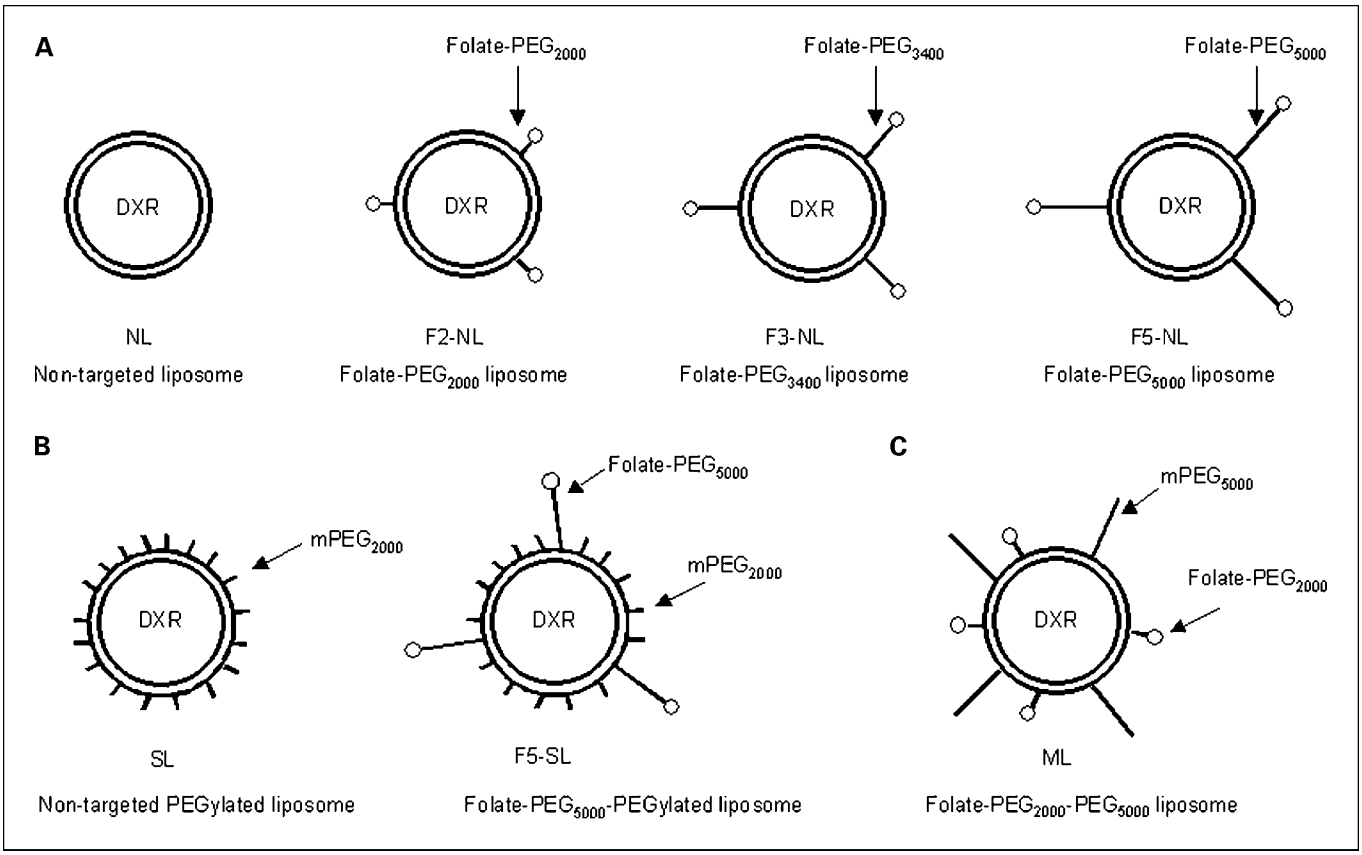

Fig. 1. Schematic diagrams of folate-linked liposomal doxorubicin (*DXR*).

Murine lung carcinoma M109 cells (high FR-expressing cell line) were obtained from Division Chemotherapy (Translational Research Center), Chiba Cancer Center. M109 cells were used to evaluate the accumulation of folate-linked liposomes in tumor tissue and therapeutic effect. The cells were subcultured by employing the biogenic system of BALB/c mice.

Cellular uptake of liposomal doxorubicin assessed by flow cytometry. KB and A549 cells were incubated with liposomal doxorubicin containing 20 μg/mL doxorubicin diluted in 1 mL medium for 1 h at 37°C. In free folate competition studies, 1 mmol/L folic acid was added to the medium. After incubation, the cells were washed with cold PBS (pH 7.4) three times, detached with 0.02% EDTA-PBS for KB cells and with 0.05% trypsin for A549 cells, and then suspended in PBS containing 0.1% bovine serum albumin and 1 mmol/L EDTA. The suspended cells were directly introduced into a FACSCalibur flow cytometer (Becton Dickinson) equipped with a 488 nm argon ion laser. Data for 10,000 fluorescent events were obtained by recording forward scatter, side scatter, and 585/42 nm fluorescence. The autofluorescence of cells incubated with medium without drugs for 1 h was taken as a control.

Confocal laser scanning microscopy. After incubation with liposomes containing 20 μg/mL doxorubicin for 1 h, the medium was removed, and the cells were washed three times with PBS and fixed with 10% formaldehyde PBS at 37°C for 20 min. Then, the cells were coated with Aqua Poly/Mount (Polyscience) to prevent fading and covered with coverslips. The fixed cells were observed with a Radiance 2100 confocal laser scanning microscope (Bio-Rad).

In vitro *cytotoxicity study.* KB cells were incubated with liposomal doxorubicin containing 0.02 to 100 μg/mL doxorubicin diluted in 100 μL medium for 2 h at 37°C. After incubation, the cells were washed with cold PBS (pH 7.4) and cultured in fresh medium for 48 h. Then, 10 μL WST-8 (Dojindo Laboratories) stock solution (5 mmol/L) was added to each well, and the plate was incubated for 1 h at 37°C. Cell viability was assessed by measuring the absorbance at 450 nm.

Pharmacokinetic analysis. Male ddY mice (body weight, ~28 g) were obtained from Tokyo Laboratory Animal Science. Liposomes were injected as a single intravenous bolus via the lateral tail vein at a dose of 5 mg/kg doxorubicin. At 3, 6, and 24 h after the injection, blood was collected and centrifuged to obtain serum. Serum doxorubicin levels were determined by a high-performance liquid chromatography method (24). The high-performance liquid chromatography system was composed of a LC-10AS pump (Shimadzu), a SIL-10A autoinjector (Shimadzu), a RF-10A_{XL} fluorescence detector (excision, 482 nm; emission, 550 nm; Shimadzu), and a YMC-Pack ODS-A, 150 × 4.6 mm i.d. column (YMC). The mobile phase was 0.1 mol/L ammonium formate (pH 4.0)/acetonitrile [7:3 (v/v)] with a flow rate of 1.0 mL/min. The concentration of doxorubicin in each sample was determined using a calibration curve, with daunomycin as the internal standard. Pharmacokinetic variables were calculated using a bootstrap method, including area under the concentration curve (from 3 to 24 h; AUC) and clearance (25).

Microscopic imaging of tumor section. M109 cells were inoculated subcutaneously into female CDF_1 mice (5 weeks old; Sankyo Lab Service). When the tumor volume reached ~100 mm^3, each preparation of liposomes, SL, 0.25F5-SL, ML, and free doxorubicin, was injected intravenously at 5 mg/kg doxorubicin body weight. Twenty-four hours after liposome injection, the mice were sacrificed, and tumor tissues were collected and immediately frozen in dry ice. The tumors were embedded in OCT compound (Tissue-Tek; Sakura Finetechnical) and processed by frozen sectioning at 10 μm. Each frozen section was mounted on a MAS-coated slide glass (SUPERFROST; Matsunami). The specimens were fixed in 4% paraformaldehyde for 15 min at room temperature and washed three times with

PBS-0.02% Tween 20. Protein blocking was done for 30 min at room temperature using PBS-0.02% Tween 20 containing 0.3% skimmed milk, and the specimens were then washed three times with PBS-0.02% Tween 20. The specimens were incubated with biotin-conjugated rat anti-mouse CD31 (PECAM-1) monoclonal antibody (BD Biosciences Pharmingen), diluted 1:200, for 1 h at room temperature and subsequently washed three times with PBS-0.02% Tween 20. Immunofluorescent staining was done by using streptavidin-FITC (Invitrogen), diluted to 1:200, for 1 h at room temperature. The specimens were washed for a final time with PBS-0.02% Tween 20, and coverslips were mounted on the glass slides with prolong Antifade (Aqua Poly/Mount; Polysciences). The specimens were examined microscopically using an ECLIPSE TS100 microscope (Nikon).

Therapeutic studies. M109 cells were inoculated subcutaneously into female CDF_1 mice (5 weeks old; Sankyo Lab Service). When the tumor volume reached ~100 to 200 mm^3, each preparation of liposomes was injected intravenously at 8 or 10 mg/kg doxorubicin body weight. Liposomal doxorubicin or free doxorubicin solution was injected via a lateral tail vein. The control group was injected with saline (0.1 mL/10 g body weight). Tumor volumes and body weight were measured at regular intervals. The tumor size was measured with vernier calipers. Tumor volume was calculated using the following equation: volume = $\pi / 6 \times LW^2$, where L is the long diameter and W is the short diameter. The animal experiments were done with ethical approval from the Institutional Animal Care and Use Committee at Hoshi University.

Statistical analysis. The statistical significance of the data was evaluated by analysis of Student's t test. $P \leq 0.05$ was considered significant.

Results and Discussion

We supposed that active targeting by folate modification could be achieved based on success in passive targeting of drug carriers by PEGylation. To optimize folate presentation, the design of folate-linked liposomes used in this study is presented in Fig. 1. We prepared three kinds of folate-linked liposomes: overhanging folate-linked NL and SL and masking folate-linked ML. For overhanging folate-linked liposomes, we used various concentrations and PEG spacer lengths of F-PEG-DSPE to attain high-affinity binding. Accordingly, liposomal formulations were characterized for their *in vitro* efficacy of drug delivery and for their *in vivo* pharmacokinetics and tumor therapeutic efficacy. Optimal formulation of folate-linked liposomes was achieved by optimizing the folate ligand density and PEG spacer length on the surface of the liposomes.

Preparation of folate-linked liposomal doxorubicin. For efficient drug delivery to the target site, drugs should be stably entrapped in liposomes. In this study, the sequence of processes of folate modification on the liposome and doxorubicin loading was examined to efficiently encapsulate doxorubicin in liposomes. We used three kinds of procedures: (A), (*a*) folate modification on liposomes, (*b*) pH gradient by changing the outside pH, and (*c*) doxorubicin loading; (B), (*a*) pH gradient by changing the outside pH, (*b*) doxorubicin loading, and (*c*) folate modification on liposomes; (C), (*a*) pH gradient by changing the outside pH, (*b*) folate modification on liposomes, and (*c*) doxorubicin loading. The liposomes prepared using procedures (A) to (C) exhibited 95%, 15.6%, and 7.3% entrapment efficiencies of doxorubicin, respectively. This finding suggested that folate modification on liposomes affected the liposomal membrane, resulting in a decrease in the pH gradient and then a decrease in the entrapment of doxorubicin. Doxorubicin loading after folate modification gave a high entrapment efficiency of >95% at a drug-to-total lipid ratio of 1:5 (w/w), corresponding with the previous report (26). Hereafter, we used procedure (A) for doxorubicin entrapment. In all cases, the average particle diameter of each liposome was ~100 nm with a narrow, monodisperse distribution and ζ potential of -9 to -14 mV.

Effect of F-PEG-DSPE in folate-linked liposomal doxorubicin on cellular uptake and drug release. First of all, the time dependency of the amount of folate-linked liposomes associated with the cells was evaluated by fluorescence of doxorubicin in cells (Supplementary Fig. S1). Flow cytometry analysis showed a shift in the curve, indicating a clear increase in cellular association of folate-linked liposomes after incubation. Until the second hour of incubation, the cellular association of folate in F5-NL increased with the increasing amount of folate more than NL. The associated amount of doxorubicin in F5-NL reached a plateau after 2 to 3 h. Because folate-linked liposomes rapidly associate with FR overexpressed KB cells, it was clarified that typical saturation was achieved within the second hour of incubation (27). Thereafter, incubation for 1 h was used in the following experiments.

Next, we examined the optimal concentration and PEG spacer length of F-PEG-DSPE in liposomes for cellular uptake. For the influence of the PEG spacer length to uptake, a larger PEG spacer, F-PEG_{5000}-DSPE, showed higher association after a 1 h incubation (Fig. 2A). With regard to the density of F-PEG-DSPE, the highest level of folate modification (0.5 mol%) showed the highest uptake regardless of PEG spacer length except for F5-NL. F5-NL with 0.25 mol%

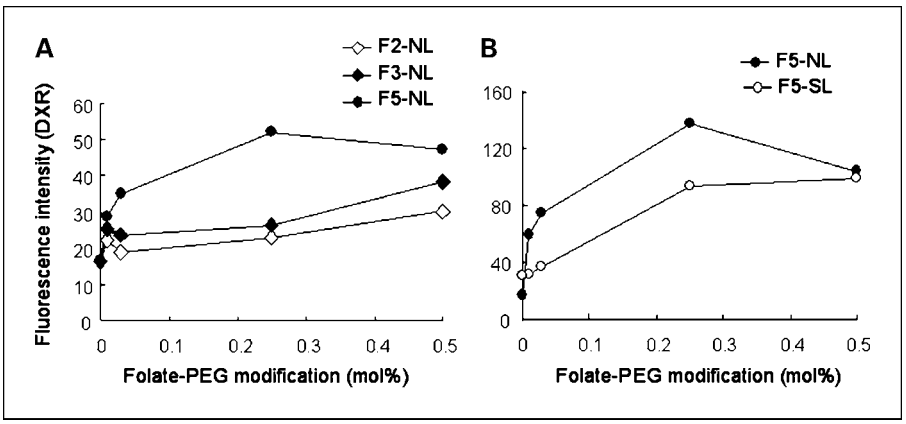

Fig. 2. Dependency of cellular association of non-PEGylated (*A*) and PEGylated (*B*) liposomal doxorubicin on folate-PEG concentration. Cell-associated doxorubicin was determined by flow cytometry analysis after KB cells were incubated with 20 μg/mL doxorubicin for 1 h at 37°C. Each analysis was generated by counting 10^4 cells.

Table 1. IC_{50} of folate-linked liposomal doxorubicin with KB cells

Formulation	IC_{50} (μg/mL)
Free doxorubicin	0.65
NL	2.39
0.25F5-NL	1.15
SL	3.37
0.03F5-SL	2.70
0.25F5-SL	1.27
ML	1.62

NOTE: Mean (n = 5).

F-PEG-DSPE had the highest association rate, showing ~3-fold greater association than nontargeted liposomes (NL). Furthermore, we compared the uptake of NL and SL modified with F-PEG_{5000}-DSPE, with the NL form showing the highest uptake (Fig. 2B). The association of 0.25F5-SL was reduced in comparison with 0.25F5-NL. Therefore, we selected 0.25F5-SL and 0.25F5-NL and compared with ML.

To compare cellular uptake of three types of liposomes, stability was evaluated by drug release. 0.25F5-SL, 0.25F5-NL, and ML were not leaky because <2% drug release was observed over a 8 h incubation period at 37°C (Supplementary Fig. S2). This result indicates that the quantity of folate modification did not affect the stability of liposomal doxorubicin.

Cellular uptake of 0.25F5-SL, 0.25F5-NL, and ML was examined in FR(+) KB and FR(-) A549 cells by flow cytometry. Cellular association of doxorubicin to KB cells was higher ML < 0.25F5-SL < 0.25F5-NL irrespective of the same 0.25 mol% folate modification (Supplementary Fig. S3). Additionally, these increased associations of 0.25F5-SL and 0.25F5-NL to KB cells could be completely blocked by adding 1 mmol/L free folic acid to the medium, but those of ML was not changed. Lower association of 0.25F5-SL and 0.25F5-NL to A549 cells was observed compared with that to KB cells, but similar association of ML was observed to both cells. PEG layer may disturb interaction of folate with FR; therefore, ML may be effectively masked by folate ligand because of less uptake nevertheless low concentration of PEG coating than 0.25F5-SL.

To investigate difference of cellular uptake among 0.25F5-SL, 0.25F5-NL, and ML, the intracellular localization of the liposomes was observed by confocal laser scanning microscopy. Fluorescence images of KB and A549 cells after incubation with liposomes for 1 h are shown in Supplementary Fig. S4. Doxorubicin fluorescence was detected as red color within cells. Higher cellular uptake of 0.25F5-SL and 0.25F5-NL to KB cells was observed than that to A549 cells, whereas ML was not taken up to both cells. This indicated that, similar to result from cellular uptake by flow cytometry, ML was masked efficiently to KB cells.

Effect of F-PEG-DSPE in folate-linked liposomal doxorubicin on cytotoxicity. To confirm the optimal density and PEG spacer length of F-PEG-DSPE in liposomes, the cytotoxicity with KB cells was measured using a WST-8 assay. Doxorubicin concentrations leading to 50% cell death (IC_{50}) were determined from the concentration-dependent cell viability curves. As shown in Table 1, the IC_{50} value of 0.25F5-NL was the highest at 1.15 μg/mL. PEGylated liposomal doxorubicin, SL (IC_{50}, 3.37 μg/mL), showed lower toxicity than NL (IC_{50}, 2.39 μg/mL). However, modification of PEGylated liposomes by 0.25 mol% folate (0.25F5-SL) showed ~2.7 times higher toxicity (IC_{50}, 1.27 μg/mL) than SL, giving a similar level of cytotoxicity to folate-linked liposomes (0.25F5-NL). Free doxorubicin (IC_{50}, 0.65 μg/mL) showed much higher cytotoxicity than the liposomes. However, because free doxorubicin has a rapid systemic clearance rate, liposomes, especially with FR targeting, are likely to exhibit a therapeutic advantage over free doxorubicin *in vivo*.

The cellular uptake of folate-linked liposomes was increased by a longer PEG spacer and a higher density of F-PEG-DSPE. Such an increment corresponded well with enhanced cytotoxicity. Cellular association of SL was decreased because the mPEG layers inhibited interaction with cells, resulting in a cytotoxicity reduction. The major benefits of the mPEG layer exist only *in vivo*.

These results concerning folate-PEG spacer length in both NL and SL corresponded well with the previous report evaluated by cellular binding *in vitro*, in which the conjugation of folate to a shorter PEG spacer reduced folate exposure by interference with the ability of the liposome to recognize FR (8). With regard to folate density, maximal FR-dependent uptake of both NL and SL was obtained previously with a density of 0.2 to 0.5 mol% F-PEG-DSPE (10, 17, 28, 29). Our data on cellular uptake and *in vitro* cytotoxicity indicated that 0.25 mol% F5-PEG-DSPE in liposomes was optimal for targeting to FR on KB cells. It is known that the folate molecule can form dimers, trimers, and even self-assembling tubular quartets at higher concentrations (18). Similar to other glycosyl phosphatidylinositol-anchored proteins, FR molecules exist as clusters in specialized microdomains in the plasma membrane. Because FR can only bind one molecule of folic acid (19), such self-assembled multimers of folic acid are incapable of binding to FR. Therefore, an increase in the density of folate ligand on liposomes may not increase the level of binding to FR. The targeting efficiency of folate-linked vesicles was affected by the amount of folate-PEG lipid.

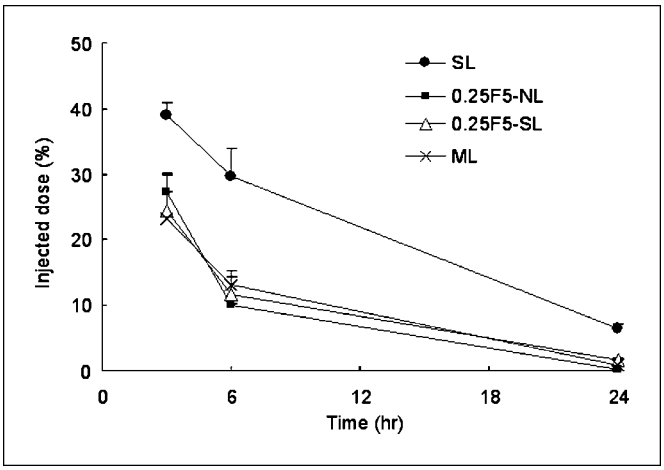

Fig. 3. Plasma concentration versus time curves of liposomal doxorubicin in mice. Liposomes were administered intravenous via tail vein injection at a dose of 5 mg/kg doxorubicin. The formulations used were SL (●), 0.25F5-SL (△), 0.25F5-NL (■), and ML (×). Mean ± SD (n = 3).

Table 2. Pharmacokinetic variables of liposomal doxorubicin in mice

Liposome	$AUC_{0\text{-}24\ h}$ (μg · h/mL)	Clearance (mL/h)
SL	491.2 ± 33.9	0.3 ± 0.02
0.25F5-NL	190.2 ± 24.2	0.7 ± 0.1
0.25F5-SL	212.1 ± 33.2	0.6 ± 0.1
ML	218.0 ± 18.4	0.6 ± 0.1

**, $P < 0.01$.

Serum doxorubicin level in mice after intravenous injection of folate-linked liposomal doxorubicin formulations. ML was designed to achieve a longer circulation time in the blood and also FR recognition on the tumor surface. The serum clearance kinetics of the various liposomal formulations in mice was compared as shown in Fig. 3 and Table 2. SL (AUC = 491.2 μg h/mL) exhibited a significantly longer circulation time than ML (AUC = 218.0 μg h/mL; clearance = 0.6 mL/h), 0.25F5-SL (AUC = 212.1 μg h/mL; clearance = 0.6 mL/h), and 0.25F5-NL (AUC = 190.2 μg h/mL; clearance = 0.7 mL/h; $P < 0.01$). Masking of the folate-linked liposomes, ML, did not achieve longer circulation times in the blood as well as 0.25F5-NL and 0.25F5-SL, as expected from the lower cellular uptake to KB cells. Our finding that 0.25F5-SL exhibited faster clearance than SL, corresponding with the previous study, indicated that the increase in folate modification of SL induced faster clearance than SL alone (9). This previous report indicated that this result was due to the distribution of folate-linked PEGylated liposomes over the internal organs, such as the liver, by the modification of folic acid (9). However, folate modification either inside or outside the mPEG-layer on the liposomes might lead to accumulation of liposomes in the tumor by FR targeting more significantly than the effect of longer circulation time. Next, we examined the distribution of folate-linked liposomal doxorubicin in tumors.

Distribution of folate-linked liposomal doxorubicin in M109 solid tumors. To evaluate the distribution of doxorubicin in

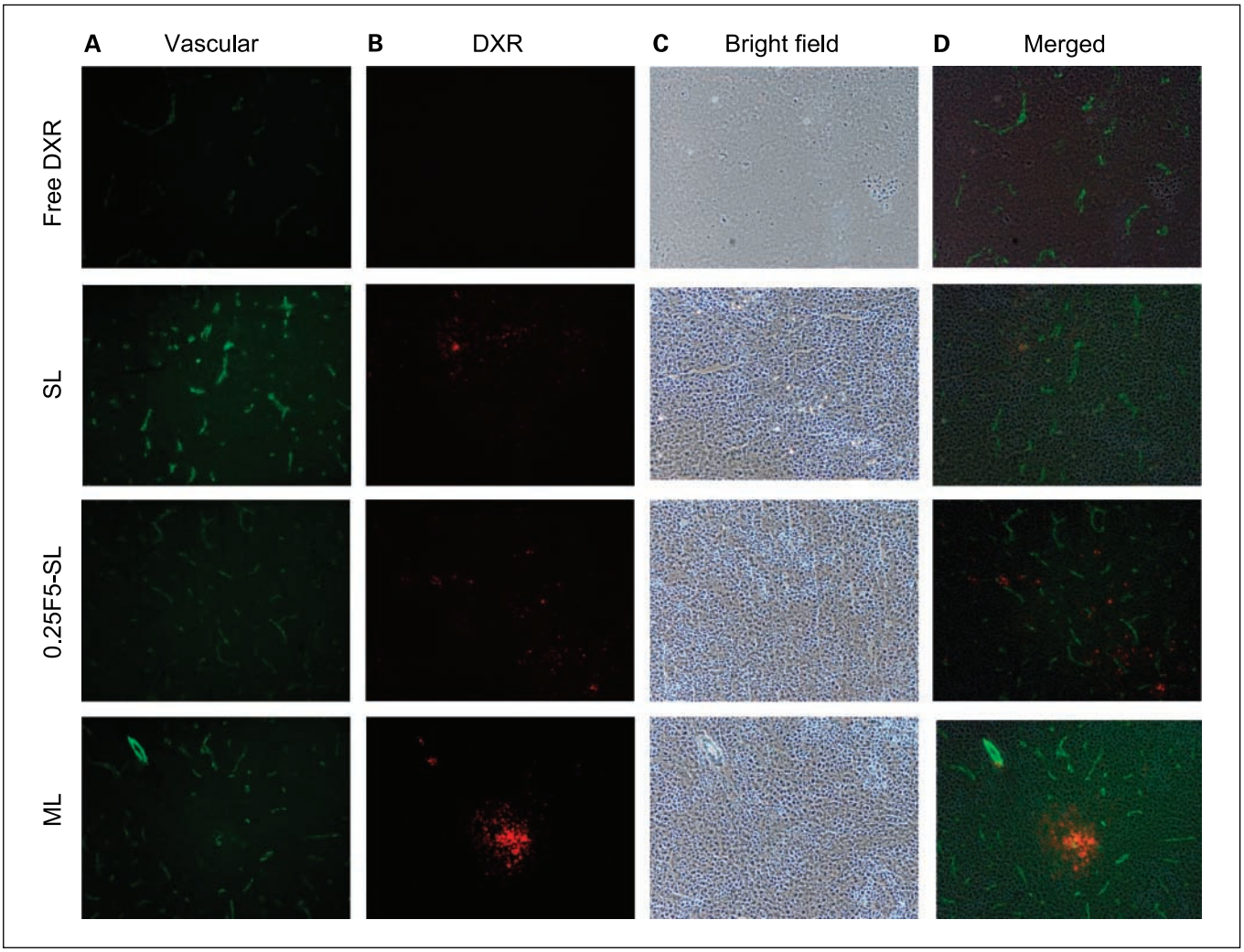

Fig. 4. Distribution of liposomal doxorubicin in M109 solid tumors measured by fluorescence microscopy. M109 cells were inoculated subcutaneously into female CDF1 mice. Twenty-four hours after intravenous administration of liposomes at a dose of 5 mg/kg doxorubicin, the tumor was excised and processed by frozen sectioning at 10 μm. Immunofluorescent staining of tumors by CD31 antibody is shown. Magnification, ×100. *Green signals,* location of neovessels; *red signals,* location of doxorubicin.

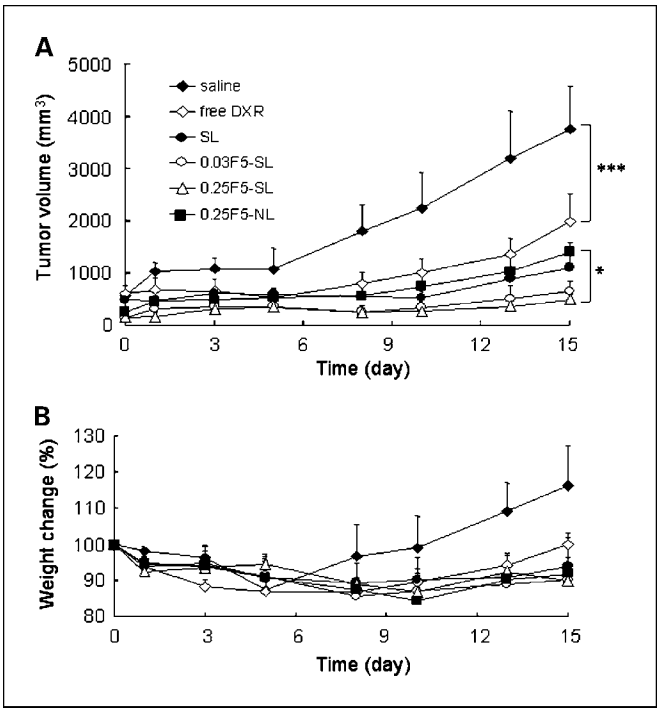

Fig. 5. Tumor growth inhibition by folate-linked liposomal doxorubicin in mice bearing M109 tumors. Tumor volume (*A*) and body weight change (*B*) after a single intravenous injection of liposomes at a dose of 10 mg/kg doxorubicin or with saline (♦). The formulations used were free doxorubicin (◇), SL (●), 0.03 F5-SL (○), 0.25F5-SL (△), and 0.25F5-NL (■). ***, $P < 0.001$; *, $P < 0.05$. Mean ± SD ($n = 6$).

tumors after intravenous injection of liposome formulations, we observed the staining of neovessels with FITC-fluorescent CD31 antibodies using a fluorescence microscope (Fig. 4). Most of the red fluorescence due to free doxorubicin was not observed in tumors 24 h later, but doxorubicin was observed in other liposome formulations. Folate-linked liposomes, ML, tended to accumulate around blood vessels, although a big difference was not seen in comparison with SL and 0.25F5-SL. This finding indicated that folate-linked liposomal doxorubicin accumulated in the tumor, whereas it did not show long circulation as SL.

Antitumor effect of folate-linked liposomal doxorubicin evaluated in M109 solid tumors. Because the folate-linked liposomes of 0.25F5-NL and 0.25F5-SL showed higher cytotoxicity than nontargeted PEGylated liposomes (SL) *in vitro*, their antitumor effect was evaluated in mice bearing M109 cells, including 0.03F5-SL and ML. At first, each preparation of liposomes (SL, 0.03F5-SL, 0.25F5-SL, and 0.25F5-NL) and free doxorubicin solution were injected intravenously at doses of 10 mg/kg doxorubicin body weight.

As shown in Fig. 5A, the doxorubicin-injected group showed a high antitumor effect in comparison with saline-treated and free doxorubicin-treated groups. The antitumor effect of folate-linked PEGylated liposomes, 0.25F5-SL, was significantly higher than that of folate-linked non-PEGylated liposomes, 0.25F5-NL, on day 15 ($P < 0.05$).

Next as shown in Fig. 6A, the antitumor effect of free doxorubicin, 0.25F5-SL, 0.25F5-NL, and SL was compared with that of ML after intravenous injection at doses of 8 mg/kg doxorubicin body weight. ML showed similar effect with 0.25F5-SL, and both liposomes showed a significantly higher antitumor effect compared with 0.25F5-NL and free doxorubicin ($P < 0.01$) but not with SL ($P > 0.05$) on day 16. SL showed a significantly higher effect with 0.25F5-NL ($P < 0.05$).

Moreover, as a result of observation of side effects by administering doxorubicin, a tendency of weight loss was seen shortly after administering free doxorubicin but not for liposomal doxorubicin (Figs. 5 and 6B). In addition, conspicuous side effects such as diarrhea were not observed with liposomal doxorubicin.

The antitumor effect of folate-linked liposomal doxorubicin, ML, and 0.25F5-SL was not significantly higher than that of SL, which was not related to the accumulation of doxorubicin in blood vessels in the tumor region (as shown in Fig. 4). This phenomenon might be ascribed to the difference in drug release rate, which is regarded as an important factor influencing the biological activity of liposomal drugs (30, 31). In order for folate-linked liposomes to bind FR in a solid tumor via intravenous injection, they require extravasation from blood vessels in the tumor region, passage through the intercellular space, and finally reach FR on the tumor cell surface. Although folate-linked liposomal doxorubicin was retained in the tumor, release of the drug into the local environment might vary. After accumulation in the tumor, SL could effectively release the encapsulated drug and free

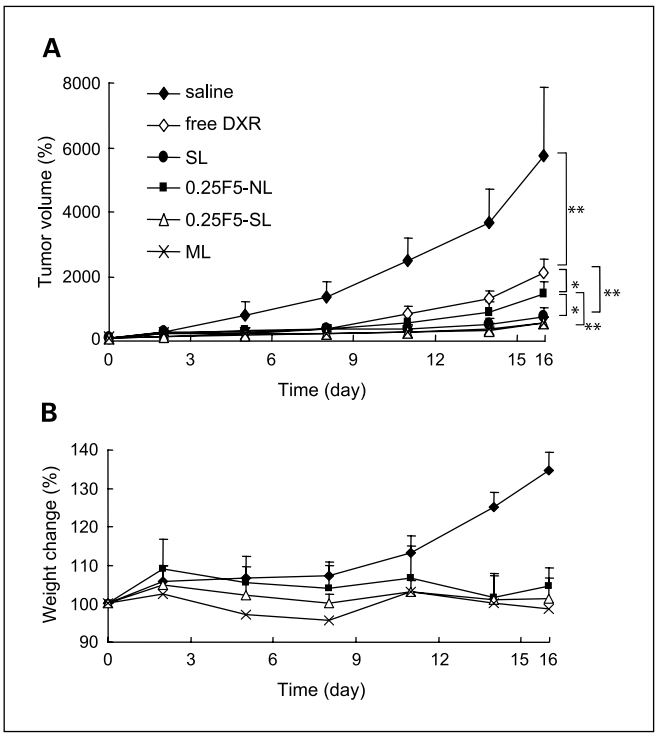

Fig. 6. Tumor growth inhibition by folate-linked and masked folate-linked liposomal doxorubicin in mice bearing M109 tumors. Tumor volume (*A*) and body weight change (*B*) after a single intravenous injection of liposomes at a dose of 8 mg/kg doxorubicin or with saline (♦). The formulations used were free doxorubicin (◇), SL (●), 0.25F5-SL (△), 0.25F5-NL (■), and ML (×). Tumor volumes are plotted as ratios to their volume before the first drug injection. Mean ± SD ($n = 6$) **, $P < 0.01$; *, $P < 0.05$.

doxorubicin rapidly reached a therapeutic concentration that can inhibit tumor growth. In contrast, ML and 0.25F5-SL could accumulate relatively highly in the tumor but could not release the required amount of drug at an appropriate rate. In a nonsolid tumor, the high therapeutic efficacy of folate-linked liposomal doxorubicin was reported in mouse ascites leukemia models, in which the treatment route was intraperitoneal injection (14). In addition, the therapeutic efficacy of intravenous treatment with folate-linked liposomal doxorubicin was improved in mice inoculated intraperitoneally with lymphoma cells (32, 33). Therefore, further study is needed for FR targeting of solid tumors by intravenous injection of folate-linked liposomes. These findings suggested that, for active targeting using folate following intravenous injection, the sterically stabilized property of liposomes was needed as well as targeting to retard tumor growth, in contrast to the *in vitro* results. Folate-linked SLs and MLs with less circulation times showed comparative antitumor effect to traditional SL. Longer linker of folate and less PEG modification will allow the design of FR targeting liposome in the clinical setting.

Conclusion

In this study, the effects of PEG spacer length and ligand density on FR-targeted liposomes were evaluated. Folate ligands with 0.25 mol% and sufficiently long PEG spacers (F-PEG_{5000}-DSPE) of NLs increased the FR association and cytotoxicity compared with those of SLs and MLs *in vitro*. On the contrary, folate-linked SLs and MLs showed a higher tumor-killing effect than folate-linked NLs *in vivo*. Further study to optimize PEG coating for FR-targeting particles will improve the antitumor effect.

Disclosure of Potential Conflicts of Interest

No potential conflicts of interest were disclosed.

References

1. Weitman SD, Lark RH, Coney LR, et al. Distribution of the folate receptor GP38 in normal and malignant cell lines and tissue. Cancer Res 1992;52:3396–401.
2. Wu M, Gunning W, Ratnam M. Expression of folate receptor type α in relation to cell type, malignancy, and differentiation in ovary, uterus, and cervix. Cancer Epidemiol Biomarkers Prev 1999;8:775–82.
3. Elnakat H, Rantnam M. Distribution, functionality and gene regulation of folate receptor isoforms: implications in targeted therapy. Adv Drug Deliv Rev 2004; 56:1067–84.
4. Shen F, Ross JF, Wang X, Ratnam M. Identification of a novel folate receptor, a truncated receptor, and receptor type β in hematopoietic cells: cDNA cloning, expression, immunoreactivity, and tissue specificity. Biochemistry 1994;33:1209–15.
5. Ross JF, Wang H, Behm FG, et al. M. Folate receptor type β is a neutrophilic lineage marker and is differentially expressed in myeloid leukemia. Cancer 1999;85: 348–57.
6. Wang H, Ross JF, Ratnam M. Structure and regulation of a polymorphic gene encoding folate receptor type γ/γ′. Nucleic Acids Res 1998;26:2132–42.
7. Lee RJ, Low PS. Folate-mediated tumor cell targeting of liposome entrapped doxorubicin *in vitro*. Biochim Biophys Acta 1995;1233:134–44.
8. Gabizon A, Horowitz AT, Goren D, et al. Targeting folate receptor with folate linked to extremities of poly (ethylene glycol)-grafted liposomes: *in vitro* studies. Bioconjug Chem 1999;10:289–98.
9. Gabizon A, Horowitz AT, Goren D, et al. *In vivo* fate of folate-targeting polyethylene-glycol liposomes in tumor-bearing mice. Clin Cancer Res 2003;9:6551–9.
10. Goren D, Horowitz AT, Tzemach D, et al. Nuclear delivery of doxorubicin via folate-targeted liposomes with bypass of multidrug-resistance efflux pump. Clin Cancer Res 2000;6:1949–57.
11. Sudimack J, Lee RJ. Drug targeting via the folate receptor. Adv Drug Deliv Rev 2000;41:147–62.
12. Hofland HE, Masson C, Iginla S, et al. Folate-targeted gene transfer *in vivo*. Mol Ther 2002;5: 739–44.
13. Pan XQ, Zheng X, Shi G, et al. A strategy for the treatment of acute myelogenous leukemia based on folate receptor type-targeted liposomal doxorubicin combined with receptor induction using all-*trans*-retinoic acid. Blood 2002;100:594–602.
14. Pan XQ, Wang H, Lee RJ. Antitumor activity of folate receptor-targeted liposomal doxorubicin in a KB oral carcinoma murine xenograft model. Pharm Res 2003; 20:417–22.
15. Rait AS, Pirollo KF, Xiang L, Ulick D, Chang EH. Tumor-targeting, systemically delivered antisense HER-2 chemosensitizes human breast cancer xenografts irrespective of HER-2 levels. Mol Med 2002; 8:475–86.
16. Zhao X, Lee RJ. Tumor-selective targeted delivery of genes and antisense oligodeoxyribonucleotides via the folate receptor. Adv Drug Deliv Rev 2004;56: 1193–204.
17. Reddy JA, Abburi C, Hofland H, et al. Folate-targeted, cationic liposome-mediated gene transfer into disseminated peritoneal tumors. Gene Ther 2002;9: 1542–50.
18. Ciuchi F, Di Nicola G, Franz H, et al. Self-recognition and self-assembly of folic acid salts: columnar liquid crystalline polymorphism and the column growth process. J Am Chem Soc 1994;116:7064–71.
19. Antony AC, Utley C, Van Horne KC, Kolhouse JF. Isolation and characterization of a folate receptor from human placenta. J Biol Chem 1981;256:9684–92.
20. Shiokawa T, Hattori Y, Kawano K, et al. Effect of polyethylene glycol linker spacer length of folate-linked microemulsions loading aclacinomycin A on targeting ability and antitumor effect *in vitro* and *in vivo*. Clin Cancer Res 2005;11:2018–25.
21. Hayama A, Yamamoto T, Yokoyama M, et al. Polymeric micelles modified by folate-PEG-lipid for targeted drug delivery to cancer cells *in vitro*. J Nanosci Nanotech 2008;8:1–8.
22. Uster PS, Allen TM, Daniel BE, et al. Insertion of poly(ethylene glycol) derivatized phospholipid into pre-formed liposomes results in prolonged *in vivo* circulation time. FEBS Lett 1996;386:243–46.
23. Lee RJ, Wang S, Turk MJ, Low PS. The effects of pH and intraliposomal buffer strength on the rate of liposome content release and intracellular drug delivery. Biosci Rep 1998;18:69–78.
24. Matsushita Y, Iguchi H, Kiyosaki T, et al. A high performance liquid chromatographic method of analysis of 4′-*O*-tetrahydropyranyladriamycin and their metabolites in biological samples. J Antibiot (Tokyo) 1983; 36:880–6.
25. Takemoto S, Yamaoka K, Nishikawa M, Takakura Y. Histogram analysis of pharmacokinetic parameters by bootstrap resampling from one-point sampling data in animal experiments. Drug Metab Pharmacokinet 2006;21:458–64.
26. Li X, Hirsh DJ, Cabral-Lilly D, et al. Doxorubicin physical state in solution and inside liposomes loaded via a pH gradient. Biochim Biophys Acta 1998;1415: 23–40.
27. Paulos CM, Reddy JA, Leamon CP, et al. Ligand binding and kinetics of folate receptor recycling *in vivo*: impact on receptor-mediated drug delivery. Mol Pharmacol 2004;66:1406–14.
28. Saul JM, Annapragada A, Natarajan JV, Bellamkonda RV. Controlled targeting of liposomal doxorubicin via the folate receptor *in vitro*. J Control Release 2003;92:49–67.
29. Shmeeda H, Mak L, Tzemach D, et al. Intracellular uptake and intracavitary targeting of folate-conjugated liposomes in a mouse lymphoma model with up-regulated folate receptors. Mol Cancer Ther 2006;5: 818–24.
30. Cui J, Li C, Guo W, et al. Direct comparison of two pegylated liposomal doxorubicin formulations: is AUC predictive for toxicity and efficacy? J Control Release 2007;118:204–15.
31. Lim HJ, Masin D, Madden TD, Bally MB, Influence of drug release characteristics on the therapeutic activity of liposomal mitoxantrone. J Pharmacol Exp Ther 1997;281:566–73.
32. Gabizon A, Shmeeda H, Horowitz AT, Zalipsky S. Tumor cell targeting of liposome-entrapped drugs with phospholipid-anchored folic acid-PEG conjugates. Adv Drug Deliv Rev 2004;56:1177–92.
33. Shmeeda H, Mak L, Tzemach D, Astrahan P, Tarshish M, Gabizon A. Intracellular uptake and intracavitary targeting of folate-conjugated liposomes in a mouse lymphoma model with up-regulated folate receptors. Mol Cancer Ther 2006;5:818–24.

Clinical Cancer Research

Design of Folate-Linked Liposomal Doxorubicin to its Antitumor Effect in Mice

Atsushi Yamada, Yukimi Taniguchi, Kumi Kawano, et al.

Clin Cancer Res 2008;14:8161-8168.